Electronic Supplementary Material (ESI) for Soft Matter.

Supplement to:

Lubricated steady sliding of a rigid sphere on a soft elastic substrate: hydrodynamic friction in the Hertz limit

Haibin Wu[a], Nichole Moyle[b], Anand Jagota[b] and Chung-Yuen Hui*[a]

[a] Department of Mechanical and Aerospace Engineering, Field of Theoretical and Applied Mechanics, Cornell University, Ithaca, NY 14853, USA

[b] Departments of Bioengineering and of Chemical & Biomolecular Engineering, 111 Research Drive, Lehigh University, Bethlehem, PA 18015, USA

1. Derivation of Reynold Equation for steady sliding

The derivation of Reynold equation can be found in the reference [1]. We use a different coordinate system compared with the standard approach. In our approach, $z=0$ corresponds to the position of the undeformed surface. The Navier-Stokes equation, ignoring inertia terms and using the lubrication approximation is:

$$\begin{aligned} &p_{,x} = \eta v_{x,zz} \\ &p_{,y} = \eta v_{y,zz} \\ &p_{,z} \approx 0 \Rightarrow p = p(x,y,t) \text{ independent of } z \end{aligned} \tag{S1a-c}$$

where p is hydrodynamic pressure; η is the constant dynamic viscosity of the liquid; v_x and v_y are velocities in the x and y direction. The lubrication approximation is that in plane gradients of the horizontal velocities are small in comparison with the out of plane gradients. Integrating (S1a,b),

$$\begin{aligned} v_x &= \frac{p_{,x}}{2\eta} z^2 + A_1(x,y,t) z + B_1(x,y,t) \\ v_y &= \frac{p_{,y}}{2\eta} z^2 + A_2(x,y,t) z + B_2(x,y,t) \end{aligned} \tag{S2a,b}$$

For our case, the equation of the rigid surface is $h(x,y,t)$ and we have:

$$v_x\left(z = h(x,y,t)\right) = v \qquad \text{and} \qquad v_x\left(z = w(x,y,t)\right) \approx 0 \tag{S3a,b}$$

$$v_y\left(z = h(x,y,t)\right) = 0 \qquad\qquad v_y\left(z = w(x,y,t)\right) \approx 0 \tag{S3c,d}$$

where v is the horizontal velocity of translation of the surface and $w(x,y,t)$ is the vertical elastic displacement of the substrate surface due to the unknown fluid pressure p. The boundary condition (S3a,b) allows us to determine the unknown functions in (S2a).

$$v_x = \left\{ \frac{p_{,x}}{2\eta}(z-h) + \frac{v}{(h-w)} \right\}(z-W)$$
$$v_y = \frac{p_{,y}}{2\eta}(z-w)(z-h) \qquad \text{(S4a,b)}$$

Finally, the incompressibility condition implies that

$$v_{z,z} = -v_{x,x} - v_{y,y} \Rightarrow v_z(h) - v_z(w) = -\int_w^{h(x,y,t)} (v_{x,x} + v_{y,y})dz \qquad \text{(S5)}$$

The RHS of the (S5) are

$$\int_w^{h(x,y,t)} v_{x,x}\, dz = \left[\int_w^{h(x,y,t)} v_x dz \right]_{,x} - vh_{,x} = \left(\frac{-p_{,x}(h-w)^3}{12\eta} \right)_{,x} - \left(\frac{v}{2} \right)(h_{,x} + w_{,x})$$
$$\int_w^{h(x,y,t)} v_{y,y}\, dz = \left[\int_w^{h(x,y,t)} v_y dz \right]_{,y} = -\left(\frac{p_{,y}(h-w)^3}{12\eta} \right)_{,y} \qquad \text{(S6a,b)}$$

Substituting (S6a,b) into (S5), we get the Reynolds equation for steady sliding,

$$\left(\frac{p_{,x}(h-w)^3}{12\eta} \right)_{,x} + \left(\frac{p_{,y}(h-w)^3}{12\eta} \right)_{,y} = -\left(\frac{v}{2} \right)(h_{,x} + w_{,x}) + v_z(h) - v_z(w) \qquad \text{(S7)}$$

For steady sliding, $\dot{w}(x,y,t) = -vw_{,x}$ and (S7) becomes

$$\frac{1}{12\eta} \nabla \cdot \left[\nabla p (h-w)^3 \right] = -\left(\frac{v}{2} \right)(h_{,x} - w_{,x}) \qquad \text{(S8)}$$

We can convert the (S8) into polar coordinates using:

$$\frac{\partial f}{\partial x} = \cos\theta \frac{\partial f}{\partial r} - \frac{\sin\theta}{r} \frac{\partial f}{\partial \theta} \; ; \quad \frac{\partial f}{\partial y} = \sin\theta \frac{\partial f}{\partial r} + \frac{\cos\theta}{r} \frac{\partial f}{\partial \theta} \qquad \text{(S9a,b)}$$

The polar coordinate version of (S8) is:

$$\frac{1}{r}\frac{\partial}{\partial r}\left(\frac{1}{12\eta} r \frac{\partial p}{\partial r} \cdot u^3 \right) + \frac{1}{r}\frac{\partial}{\partial \theta}\left(\frac{1}{12\eta} \frac{1}{r} \frac{\partial p}{\partial \theta} \cdot u^3 \right) = -\frac{v}{2}\left(\cos\theta \frac{\partial u}{\partial r} - \frac{\sin\theta}{r} \frac{\partial u}{\partial \theta} \right) \qquad \text{(S10)}$$

where: $u = h - w$.

2. Resolving the singularity of the discretized Reynolds equation at $\bar{r} = 0$

To get rid of the singularity, we integrated both sides of (2.6a) in the paper over a small domain D and applied divergence theorem to obtain (2.15). We choose the domain D as a circular region centered at origin with radius $\varepsilon = \Delta\bar{r}_1 / 2$. We evaluate both sides of the (2.15) using the finite difference scheme:

$$LHS=\int_{\partial D}\bar{u}^3\frac{\partial\bar{p}}{\partial\bar{r}}ds=\sum_{\theta=0}^{\theta=\pi}\varepsilon\left(\bar{u}^3\frac{\partial\bar{p}}{\partial\bar{r}}\right)_{\bar{r}=\varepsilon,\theta}=\sum_{\theta=0}^{\theta=\pi}\frac{\Delta\bar{r}_1}{2}\left(\bar{u}^3\frac{\partial\bar{p}}{\partial\bar{r}}\right)_{\bar{r}=\frac{\Delta\bar{r}_1}{2},\theta}\cdot\Delta\theta=\sum_{i=0}^{m}\frac{\Delta\bar{r}_1}{2}\left(\frac{\bar{u}_{i,0}^3+\bar{u}_{i,1}^3}{2}\frac{\bar{p}_{i,1}-\bar{p}_{i,0}}{\Delta\bar{r}}\right)\Delta\theta \quad \text{(S11a)}$$

$$RHS=\int_0^{\pi}\int_0^{\varepsilon}\left[\frac{-1}{\beta}\left(\cos\theta\frac{\partial\bar{u}}{\partial\bar{r}}-\frac{\sin\theta}{\bar{r}}\frac{\partial\bar{u}}{\partial\theta}\right)\right]\bar{r}d\bar{r}d\theta=-\frac{1}{\beta}\sum_{i=0}^{m}\left[\frac{1}{2}\cos\theta_i\frac{\left(u_{i,1}-u_{i,0}\right)}{\Delta\bar{r}_1}\left(\frac{\Delta\bar{r}_1}{2}\right)^2\Delta\theta-\sin\theta_i\frac{\left(\bar{u}_{i+1,1/2}-\bar{u}_{i-1,1/2}\right)}{2\Delta\theta}\left(\frac{\Delta\bar{r}_1}{2}\right)\Delta\theta\right] \quad \text{(S11b)}$$

where

$$\bar{u}_{i+1,\,1/2}=\frac{\left(\bar{u}_{i+1,\,0}+\bar{u}_{i+1,\,1}\right)}{2};\ \ \bar{u}_{i-1,\,1/2}=\frac{\left(\bar{u}_{i-1,\,0}+\bar{u}_{i-1,\,1}\right)}{2}, \quad \text{(S11c)}$$

Since $\bar{p}_{i,0}$, $\bar{u}_{i,0}$ are independent of θ, we denote them by $\bar{p}_0$, u_0 respectively. Using (S11a-b), we obtain (2.16) in the paper.

3. Hydrodynamic pressure over the whole domain.

The hydrodynamic pressure at different cross sections is shown in figure 5 in the paper. The pressure profiles over the whole calculation domain for different β value are shown in figure S1.

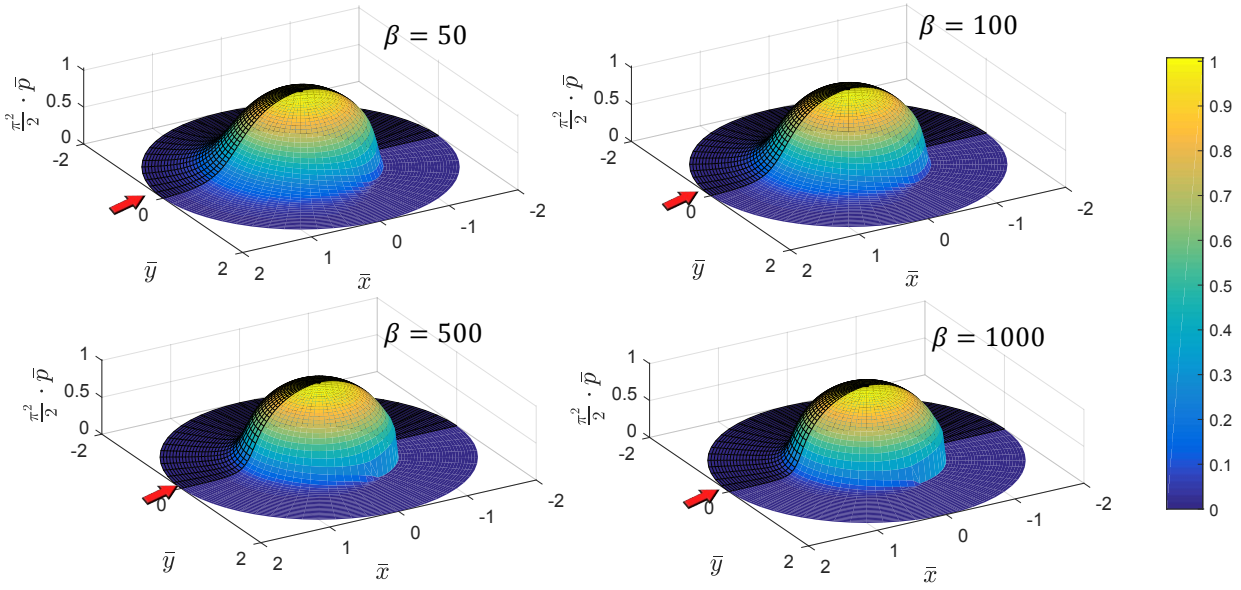

Figure S1. Pressure profile over the calculation domain for different β value

As β increase the hydrodynamic pressure become more and more axisymmetric and converges to the Hertz pressure, except near the intake and exit. For β values larger than 500, there is very little change of the pressure profile except in a small region very close to $\bar{r}=1$.

4. Displacement of the elastic substrate

The vertical displacement of the substrate at two main cross sections ($\bar{y}=0$ and $\bar{x}=0$) for different β is plotted in figure S2. Also plotted is the Hertzian solution.

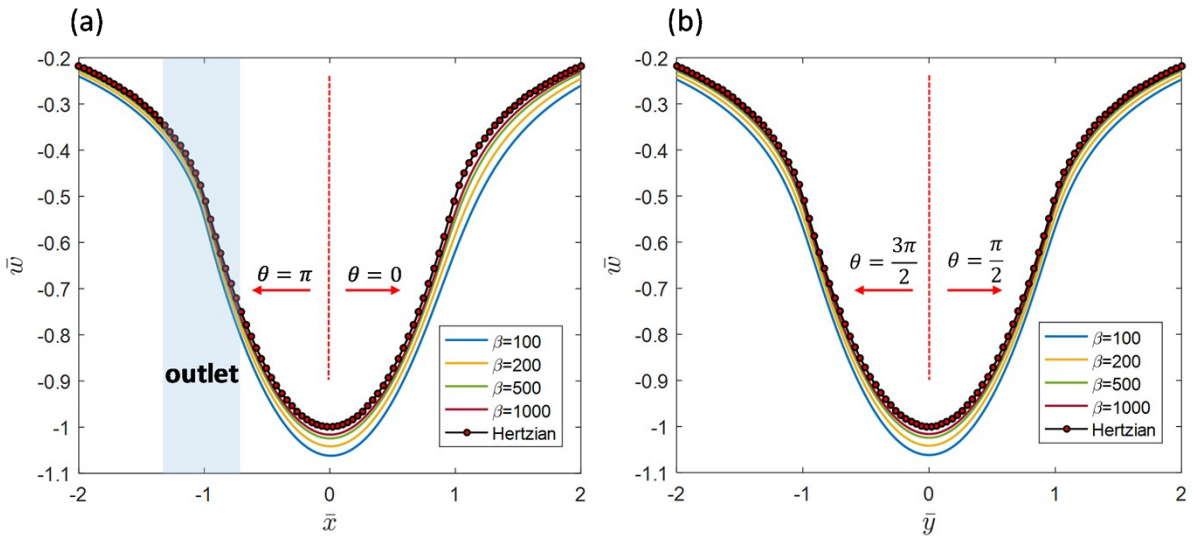

Figure S2. Substrate's displacement for different β value at different cross sections, (a) cross section at $\bar{y} = 0$; (b) cross section at $\bar{x} = 0$.

The results show that as β increases, the substrate's vertical displacement caused by hydrodynamic pressure approaches the Hertzian solution. At the exit region where $\bar{r} \approx 1$ and $\theta \approx \pi$, the vertical displacement is closer to the Hertz solution which implies a thinner film there.

5. Compare between the cavitation and non-cavitation condition

The comparison of the EHL solution with and without enforcing Reynold condition is shown in figure S3 and figure S4.

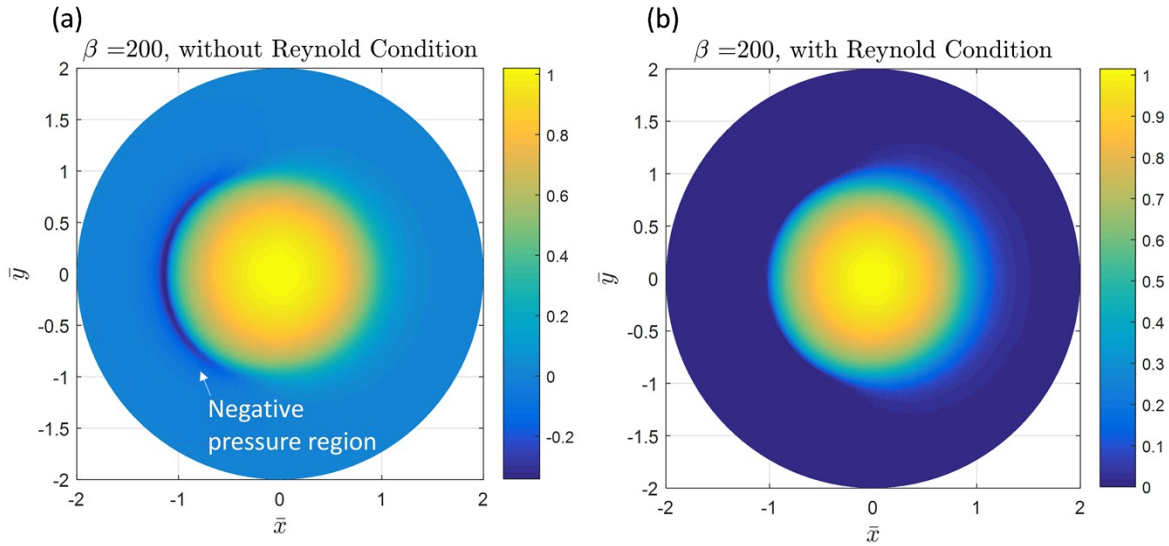

Figure S3. the comparison of hydrodynamic pressure for the calculations: (a) without Reynold condition; and (b) with Reynold condition

The comparison of hydrodynamic pressure over the calculation domain for the cases of enforcing no Reynold condition and Reynold condition is shown in shown in figure S3 for $\beta = 200$. We choose a relatively small value of β since it give a clear picture of the boundary layer effect. The result shows that unless the Reynold condition is imposed, there is always a small region near the exit where negative hydrodynamic pressure exists. The negative pressure might cause cavitation of between the liquid layer and the rigid sphere. However, both the magnitude and size of this negative pressure vanishes as $\beta \to \infty$ so it is not a concern. Indeed, since the Reynolds condition is also an approximation, it is not clear which model is better in this limit. Indeed, in our experiments, we did not observe fingering or cavitation at the exit.

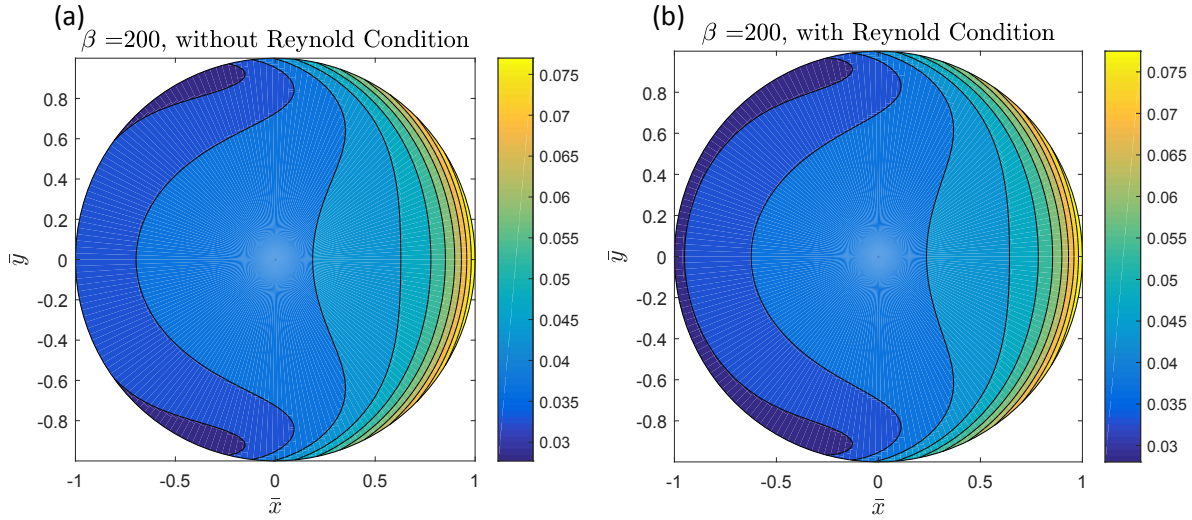

Figure S4. the comparison of hydrodynamic pressure for the calculations: (a) without Reynold condition; and (b) with Reynold condition for $\beta = 200$

The effect of Reynold condition on the distribution of the liquid film thickness is shown in figure S4 for $\beta = 200$. (a) Reynold condition is not enforced (b) Reynold condition enforced. Even for $\beta = 200$ the Reynold condition has no effect on the inlet region $\bar{x} > 0$. The effect is focused on a very small boundary layer near the exit. The presence of Reynold condition actually makes the liquid layer thinner at the exit region where $\bar{r} \approx 1, \theta = \frac{2}{3}\pi \sim \frac{4}{3}\pi$.

6. Velocity field at different cutting planes

The average velocity for the velocity components $\bar{v}_r$ and $\bar{v}_\theta$ was shown in figure 11 in the paper. Here, we presents more results of the velocity vector field in the whole calculate domain for different cutting planes.

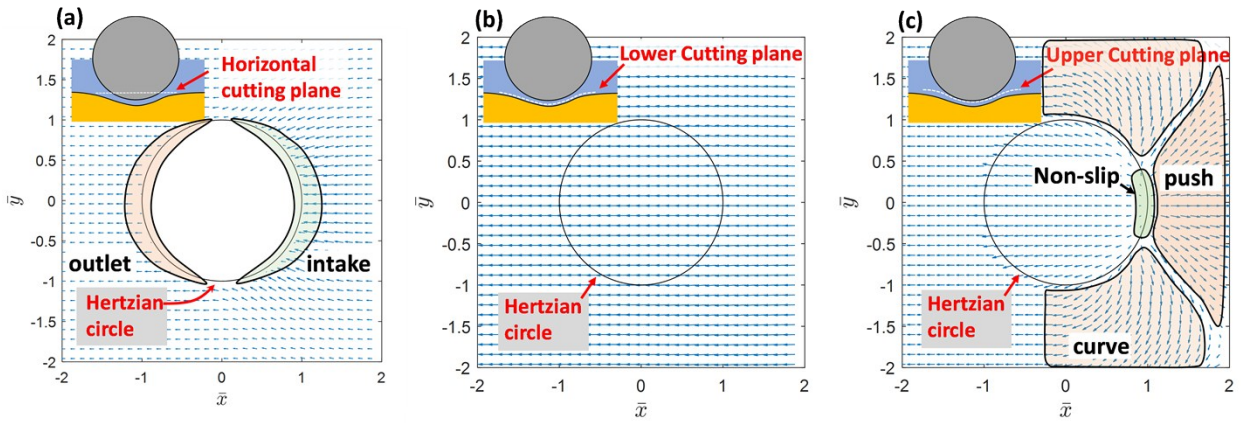

Figure S5. the velocity field at different cutting plane between the sphere and substrate

The velocity field at three horizontal cutting plane sections are shown in figure S5. With respect to the sphere, the liquid flows from left to right. figure S5(a) is a horizontal plane cutting both the liquid and the sphere. Generally, the liquid sucked into the thin-film region from the front side of the sphere and exits from the trailing-edge. Around the sphere, the flow curves slightly along with the circumference of the sphere. figure S5(b) shows the flow on a curve surface that is a rigid translation of the deformed substrate surface. The distance between this surface and the deformed substrate is 5% of the film thickness.

As shown in figure S5(b), because of the no slip boundary condition, the flow is practically uniform and is not affected by the shape of the sphere. figure S5(c) shows the same surface shifted upwards so the distance of this surface and the substrate surface is 95% of the film thickness. As shown in figure S5(c), at the front edge, the relative motion between the sphere and the liquid is almost negligible because of the no-slip condition. Right in front of this non-slip region, liquid is pushed out due to the forward motion of the sphere.

7. Comparison with results of Snoeijer et al.

A recent work by Snoeijer et al [4] focused on a 2D rigid cylinder sliding on a lubricated elastic half space. They also provided limited results for the sphere problem. Using a similar normalization as ours, they shown that all the normalized variables depends on the single dimensionless parameter λ_{3D} which within a numerical constant of order one is $\lambda_{3D} \sim \dfrac{\eta v \cos\theta R^{5/3} G^{1/3}}{N^{4/3}}$. This parameter is essentially the same as $1/\beta$ in this work. To compare our results with theirs, we plot the normalized film thickness at the inlet region $\bar{r} - 1 = 0,$ with $\theta = 0$. For this case, $\lambda_{3D} = (c\beta)^{-1}$ where $c = 0.3285$ and compare our results with their result presented in Figure 3 of their paper. As shown in Figure S6 below, there is close agreement between the two results.

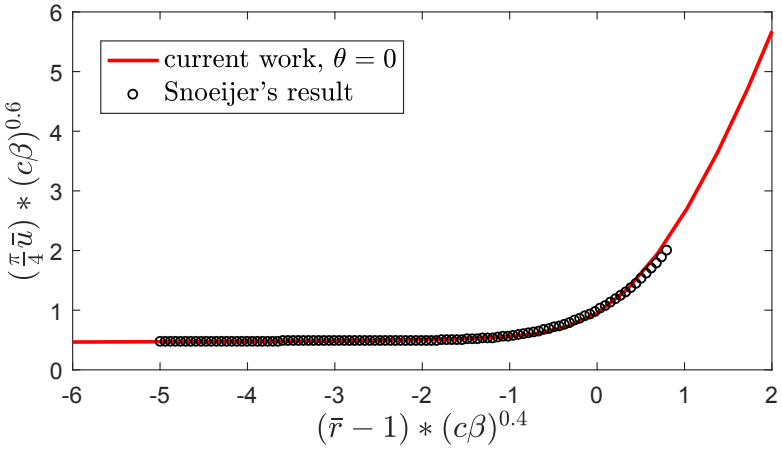

Figure S6. Comparison of current work with the asymptotic result in for the film thickness at the inlet region $\bar{r} - 1 = 0,\ \theta = 0$.

Reference

1 B. J. Hamrock, S. R. Schmid and B. O. Jacobson, *Fundamentals of fluid film lubrication*, Marcel Dekker, New York, 2nd ed., 2004.

2 B. J. Hamrock and D. Dowson, *Journal of Lubrication Technology*, 1977, **99**, 264.

3 A. P. Ranger, C. M. M. Ettles and A. Cameron, *Proceedings of the Royal Society A: Mathematical, Physical and Engineering Sciences*, 1975, **346**, 227–244.

4 J. H. Snoeijer, J. Eggers and C. H. Venner, *Physics of Fluids*, 2013, **25**, 101705.

5 J. de Vicente, J. R. Stokes and H. A. Spikes, *Tribol Lett*, 2005, **20**, 273–286.